Multilevel Thermally Assisted Magnetoresistive Random-Access Memory Based on Exchange-Biased Vortex Configurations

C. I. L. de Araujo,[1,2,3,4] S. G. Alves,[4] L. D. Buda-Prejbeanu,[1,2,3,4] and B. Dieny[1,2,3,4]

[1]*Université Grenoble Alpes, INAC-SPINTEC, F-38000 Grenoble, France*
[2]*CEA, INAC-SPINTEC, F-38000 Grenoble, France*
[3]*CNRS, SPINTEC, F-38000 Grenoble, France*
[4]*Laboratory of Spintronics and Nanomagnetism (LabSpiN), Universidade Federal de Viçosa, Viçosa, Minas Gerais 36570-900, Brazil*

(Received 25 April 2016; revised manuscript received 4 July 2016; published 23 August 2016)

A concept of multilevel thermally assisted magnetoresistive random-access memory is proposed and investigated by micromagnetic simulations. The storage cells are magnetic tunnel junctions in which the storage layer is exchange biased and in a vortex configuration. The reference layer is an unpinned soft magnetic layer. The stored information is encoded via the position of the vortex core in the storage layer. This position can be varied along two degrees of freedom: the radius and the in-plane angle. The information is read out from the amplitude and phase of the tunnel magnetoresistance signal obtained by applying a rotating field on the cell without heating the cell. Various configurations are compared in which the soft reference layer consists of either a simple ferromagnetic layer or a synthetic antiferromagnetic sandwich (SAF). Among those, the most practical one comprises a SAF reference layer in which the magnetostatic interaction between the SAF and storage layer is minimized. This type of cell should allow one to store at least 40 different states per cell representing more than five bits per cell.

DOI: 10.1103/PhysRevApplied.6.024015

I. INTRODUCTION

Since the discovery of tunnel magnetoresistance (TMR) at room temperature in magnetic tunnel junctions (MTJs) [1,2], magnetoresistive random-access memory (MRAM) technologies have been extensively investigated. In the past few years, MRAMs have been identified with resistive RAM as one of the most promising technologies of nonvolatile memories allowing downsize scalability to and beyond the 16-nm technology node. Because of their very large endurance, they are envisioned as a possible replacement to static random-access memory (SRAM), embedded Flash, and possibly DRAM at the sub-1x node. Indeed, MRAMs gather a number of advantages, since they are nonvolatile and exhibit good downsize scalability, quasi-infinite endurance, and invulnerability against ionizing radiations in hard environment applications, like aerospace or nuclear technology. Furthermore, they are compatible with CMOS technology by integrating MTJs between metallic levels of CMOS technology [3].

In MRAM devices, the storage element within each bit cell is a MTJ, which comprises two ferromagnetic layers, denominated the storage and reference layers, separated by a thin insulating layer acting as a tunnel barrier. In an in-plane magnetized MTJ, the reference-layer magnetization is usually pinned by coupling with an adjacent antiferromagnetic layer (exchange-bias phenomenon), while the storage-layer magnetization can be switched upon writing. Most of the previously developed MRAMs are for binary storage. Their two logic states ("0" and "1") correspond to two possible orientations of the storage-layer magnetization. The in-plane anisotropy yielding these two stable magnetization orientations is usually a uniaxial magnetic shape anisotropy obtained by giving to the cell an elongated elliptical shape. Each MTJ is connected in series with a selection transistor. Upon reading, the transistor is turned on so that a current can flow through the MTJ. The cell magnetic state is then assessed from the MTJ resistance value, high or low corresponding to a 1 or a 0 logical state. The MRAM technologies are divided into several schemes, which differ by their writing process. The first to stand out is the field-written toggle MRAM, using a synthetic antiferromagnetic (SAF) sandwich in the storage layer [4]. The elliptical bit cell is located between orthogonal writing lines (bit and word lines) with the long axis oriented at 45° with respect to them. To toggle the magnetization of the storage layer, a sequence of pulses of current is applied in the orthogonal writing lines, which cross each other at the addressed memory point. These pulses of current create local magnetic fields on the storage-layer magnetization in order to switch it in the desired direction. This sequence of write pulses is such that the net field acting on the storage-layer magnetization rotates by three successive steps of 45°. This applied field first induces a scissoring of the SAF storage-layer magnetization creating a net moment, which then rotates with the rotating field in three steps of approximately 45°. When the field is switched off, the SAF storage layer relaxes to its antiferromagnetic configuration along the easy axis, resulting in a 180° rotation of its

 © 2016 American Physical Society

magnetization [5]. Toggle MRAM technology provides good bit selectivity but presents a poor downsize scalability due to the large current (approximately 10 mA) required to create the magnetic-field pulses and to the associated electromigration limit in the field generating lines [5].

To lower the memory power consumption and the requirement for a large writing field of toggle MRAM, a thermally assisted writing approach is proposed (TA MRAM) [6]. This approach allows circumventing the classical dilemma in storage technology between the stability of the written information (retention) and the memory writability [7]. The approach consists in temporarily heating the memory element upon write so as to reduce the energy barrier separating the two memory states. Once heated, the storage-layer magnetization is switched with a low field (approximately 5 mT). After magnetization switching, the cell cools back to its standby temperature, where the energy barrier recovers its large value. This approach has been mostly implemented with an in-plane magnetized storage layer. In this case, the storage layer is advantageously coupled to an antiferromagnetic (AFM) layer [7]. Because of the phenomenon of exchange bias, the storage-layer magnetization is pinned by the adjacent AFM layer up to the AFM blocking temperature. Above this temperature, the storage-layer magnetization is no longer pinned and can be easily switched by an applied field. Since the storage-layer magnetization is here pinned by the adjacent AFM layer, there is no need to give to the cell an elliptical shape. Consequently, in TA MRAM, the cells can be circular. The AFM coupled to the storage layer is chosen with a blocking temperature lower than the AFM pinning the reference layer (typically, 200 °C versus 350 °C), so that, upon heating at about 220 °C, the storage-layer magnetization can be switched whereas the reference-layer magnetization always remains in the same state. During the writing process, the transistor is turned on to generate a current through the MTJ, thus heating the storage layer up to the AFM blocking temperature. Thanks to the circular shape of the bit cells and correlative absence of shape anisotropy, only a weak magnetic field of a few milliteslas is then sufficient to switch the storage-layer magnetization [8]. The TA-MRAM power consumption can be further reduced by sharing the field pulse between all bits of a given word [8]. This, however, remains a field-written technology and therefore has also a limited downsize scalability albeit better than that of toggle MRAM because of the lower write field and field sharing.

However, nowadays, the mainstream MRAM technology is based on spin-transfer-torque writing (STT MRAM), a phenomenon independently predicted by Slonczewski and Berger [9,10], not requiring any field line. When the transistor is turned on, an applied current flows through the MTJ. The tunneling current is spin polarized due to the magnetic nature of the reference metallic electrode. The spin-polarized electrons then tunnel through the tunnel barrier and, due to their exchange interactions with those responsible for the local magnetization, exert a torque on the storage-layer magnetization [9]. If the current is large enough, the storage-layer magnetization then switches parallel or antiparallel to the reference-layer magnetization depending on the current direction through the stack (upwards or downwards). STT-induced switching in MTJs was first observed in 2004 [11]. STT MRAM offers much better downsize scalability than field-written MRAM, especially STT MRAM based on out-of-plane magnetized MTJs [3]. However, the fact that, at each write event, the tunnel barrier is exposed to a significant voltage pulse (approximately 0.5 V) can cause reliability and endurance problems [12,13]. This becomes more critical if one tries to increase the switching speed to address, for instance, SRAM-type applications. Indeed, the faster the switching, the larger the voltage pulse has to be, especially below typically a 5-ns write pulse [3]. To circumvent this problem, another write approach based on spin-orbit-torque switching was recently proposed [14–18]. This approach seems promising for high-speed operation. However, due to the larger footprint associated with the three-terminal geometry, it does not allow high density.

In all the schemes described above, the memories have only two states per bit. These MRAMs are intended for binary storage. A multilevel concept of STT MRAM consisting in stacking several MTJs was proposed, but the implementation in real products looks extremely challenging due to very narrow margins and reduced performances in terms of write and read speed [19].

A multilevel storage approach in TA MRAM was also proposed based on the possibility, thanks to the use of an exchange-biased storage layer, to set the storage-layer magnetization not only in two opposite directions along an easy axis but in any in-plane direction. Multilevel storage can then be achieved by applying the write field in one of a number of predetermined in-plane directions, as presented in Fig. 1(a), thanks to the use of two sets of orthogonal field-generation lines (bit lines and word lines) similar to those of toggle MRAM [20].

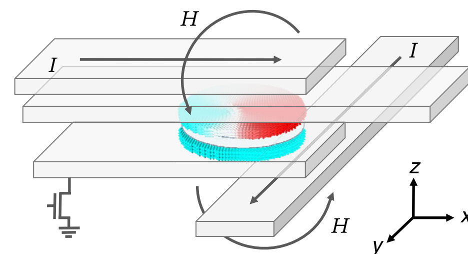

FIG. 1. Structure of multilevel TA MRAM. The upper disk represents the storage layer in the vortex configuration. The lower disk represents the reference layer which is here in a single-domain state. The color code is related to the in-plane orientation of the magnetization. The two field-generating lines (above and below the MTJ) allow creating an in-plane field in any in-plane direction.

This concept has been experimentally demonstrated using single-domain storage and reference layers. The capability to store eight or 16 different states per cell (i.e., three or four bits per cell) is demonstrated [21]. In such an approach, it is advantageous to use a soft reference layer for reading out the stored information. This means that, instead of being pinned as in conventional MRAM, the reference layer is made of an unpinned soft magnetic material, so that its magnetization can be easily rotated with a weak rotating applied field. Upon read, a rotating field is generated by combining two sinusoidal currents 90∘ out of phase in the bit and word lines. The rotation of the soft reference layer yields an approximately sinusoidal variation of the MTJ conductance whose phase indicates the direction of the storage-layer magnetization and therefore the stored information.

In this work, we investigate the possibility to go even further in multilevel storage thanks to the use of a magnetic vortex configuration in the storage layer [22]. As demonstrated by Sort *et al.* [23], it is possible to imprint an exchange-biased vortex configuration in ferromagnetic and antiferromagnetic bilayers patterned in a disk shape by cooling the bilayer from the AFM blocking temperature while the ferromagnetic-layer magnetization is in a vortex configuration. If the system is zero field cooled, the vortex core is located at the center of the disk and pinned in this configuration. However, if the system is cooled under a magnetic field lower than the vortex annihilation field, then the vortex can be pinned in an asymmetric configuration wherein the position of the vortex core is shifted transversally to the direction of the applied field at a radius which depends on the field amplitude, exchange stiffness, magnetization, and disk geometry [23]. This allows developing an alternative multilevel TA-MRAM approach in which the information is encoded via the core vortex position in the storage layer with two control parameters: the radius and angle of the vortex core position. Concerning the soft reference layer, depending on its chosen thickness, its magnetization can be either in a vortex configuration or in a uniform in-plane configuration. In both cases, the readout can be performed by applying a rotating field. This field acts mainly on the soft reference-layer magnetization, since the storage-layer magnetization is pinned by exchange bias at the standby temperature. Then by analyzing the phase and amplitude of the oscillation of MTJ conductance during the field rotation, one can assess at which angle and radius the core vortex is located in the storage layer and thus determine the corresponding logic state. In this study, we investigate the feasibility of this multilevel storage approach by micromagnetic simulations. We show that the proposed approach can enable the storage of at least 40 states per cell, equivalent to more than five bits per cell.

The micromagnetic simulations are performed with the Mumax^3 code [24]. The material parameters used are representative of CoFe, i.e., saturation magnetization $M_s = 1.4\times10^6$ A/m, exchange stiffness $A_{\mathrm{ex}} = 1.5\times10^{-11}$ J/m, and damping constant $\alpha = 0.03$. With these values, the exchange length $L_{\mathrm{ex}} = \sqrt{2A_{\mathrm{ex}}/[\mu_0 M_s^2]}$ is equal to 3.5 nm. The mesh size is $3\times3\times1$ nm. To describe the exchange bias, the chosen parameter for the FM/AFM exchange-bias interaction is representative of Co alloy/IrMn bilayers characterized by an interfacial exchange energy per unit area of $J_{\mathrm{ex}} = 0.36\ \mathrm{mJ/cm^2}$ [25]. With this value, assuming a storage-layer thickness $t = 3$ nm, a resulting exchange-bias field of $H_{\mathrm{ex}} = 80$ mT is derived using the following expression:

$$H_{\mathrm{ex}} = \frac{J_{\mathrm{ex}}}{M_s t}. \quad (1)$$

Our study is conducted assuming a cell diameter of 150 nm, which is in the range of cell size generally used in field-written MRAM (toggle [5] or TA MRAM [6]). This corresponds to a radius-to-exchange length ratio $R/L_{\mathrm{ex}} = 21.5$. According to Ref. [22], for this R/L_{ex} ratio, an equilibrium ground state of the storage layer at zero field corresponding to a vortex state is obtained for a thickness-to-exchange length ratio L/L_{ex} of the order of 1.74, meaning a thickness of the storage layer of $L = 6$ nm. This would, however, be excessively thick for our foreseen application for two reasons: (i) the exchange-bias field decreases inversely proportional to the layer thickness and would be too weak to allow pinning the vortex core in a strongly asymmetric position upon field cooling, and (ii) the vortex susceptibility in the regime $L/R \ll 1$ is expected to vary as $\chi(0) = R/\{2L[Ln(8R/L) - (\frac{1}{2})]\}$ [26], which means that, for a given applied field, the transverse vortex core shift decreases approximately inversely proportional to the layer thickness. In this multilevel storage where we seek to position the vortex core at various radii, it is preferable to maximize the vortex susceptibility and therefore minimize the storage-layer thickness. We therefore choose a storage-layer thickness L of the order of 3–4 nm. For the corresponding value L/L_{ex} between 0.86 and 1.1, the storage layer can be stabilized in two different micromagnetic states: either in the vortex state or the C state [22]. Since we want the storage layer to be in the vortex state and not in the C state, we apply an initializing procedure consisting in saturating the storage layer with an out-of-plane field of 1 T while heating up the AFM layer above its blocking temperature. Then, by gradually reducing the out-of-plane field to zero, the vortex state can be stabilized. Subsequently, the in-plane write field is applied lower than the vortex annihilation field and the cell cooled down to the standby temperature to pin the vortex state in the asymmetric configuration acquired during the field cooling. In the micromagnetic simulations, the pinning by the antiferromagnet is simulated by locally applying to the magnetization of the ferromagnetic disk an exchange-bias

field H_{ex} of the amplitude given by Eq. (1) and oriented in the direction taken by the interfacial magnetization at the FM/AFM interface during the cooling procedure when traversing the AFM blocking temperature.

The soft reference-layer magnetic configuration can also be set in the vortex state by using the same thickness as for the storage layer (e.g., 3 nm) and exposing it to the same 1-T initialization out-of-plane field as for the storage layer. In addition, to make sure that the vortices in the storage layer and reference layers are both of the same chirality, a 1-mA current is assumed to be sent through the cells creating an Oersted field large enough to force all vortices to acquire the same chirality. Otherwise, the vortex chirality would not be well controlled, possibly ending in clockwise or anticlockwise configurations resulting in different responses of the cells to the same write applied field.

Alternatively, the reference layer can be made close to uniform (i.e., single domain) by choosing a thinner reference layer (approximately 1.2 nm thick). We show in this study that this configuration is more favorable in terms of the readout signal. Besides, using a thin reference layer may experimentally allow one to get less hysteresis in this soft reference layer, since its magnetization is then closer to the superparamagnetic limit. The advantage of using such a thinner layer to improve the softness of the free layer in MTJs was demonstrated, for instance, in the context of TMR sensors [27]. The drawback is, however, a reduction in the TMR amplitude [27].

II. RESULTS AND DISCUSSION

Two different configurations are compared. The storage layer is engineered to be always in the vortex state, while the soft reference layer is either in the vortex state or close to the single-domain state. These two configurations can be realized by adjusting the thickness of the soft reference layer and using different initialization conditions as described below.

A. Storage and soft reference layer both in the vortex configuration

Two different configurations are compared. In the first one, the storage layer is chosen to 4 nm thick and the reference layer 2 nm thick. In this case, after applying the out-of-plane field-cooling protocol described above and despite the presence of the Oersted field from the setting current, it is found that, in the relaxed remanent state, the two vortices have aligned core polarization but opposite chirality [Fig. 2(a)]. This can be explained by the dipolar interactions between the two vortex cores and between the in-plane components of the two vortices exceeding the Oersted field due to the setting current. In a second configuration, the reference layer and storage layer are chosen with the same thickness of 3 nm. After relaxing the structure as in the previous case, the chirality and polarization are found to be the same in both layers, as presented in Fig. 2(b). In order to study the stability of this double-vortex configuration, a full hysteresis curve [Fig. 2(c)] is simulated. In this procedure, the magnetic field is varied step by step. Between two steps, the magnetization relaxes towards the local energy minimum. From this loop, the field necessary to annihilate the vortex in the soft reference layer can be estimated to be approximately 50 mT and approximately 140 mT for the pinned storage layer. On the decreasing-field branch, it is important to note that the reference layer never switches back to the vortex state. Once the vortex is annihilated, it does not appear again with an in-plane field. This means that this configuration with two vortices of same chirality is quite metastable for these choices of thickness and that the

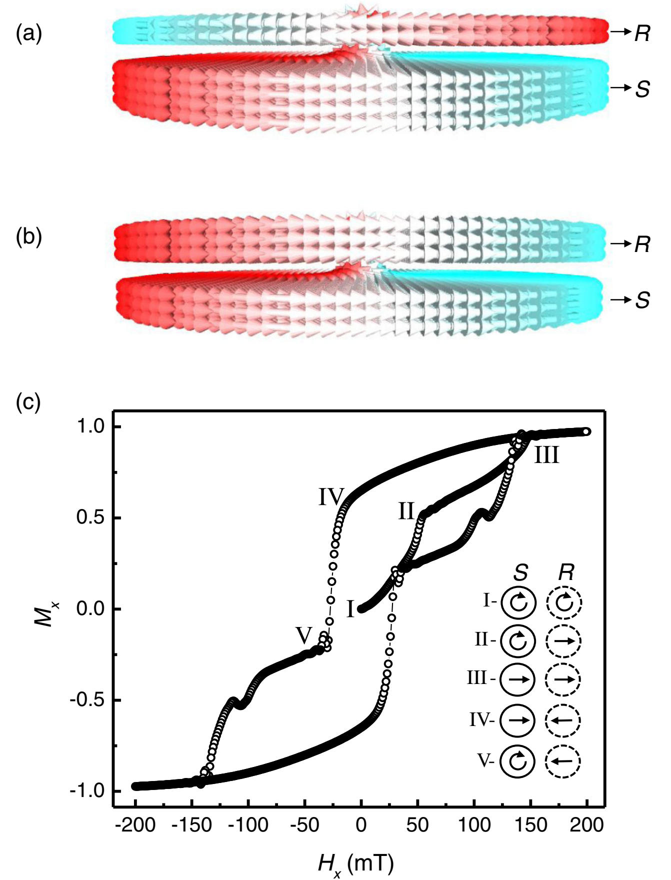

FIG. 2. Vortex configurations after the out-of-plane field-cooling protocol. (a) Structure in which the storage (S) layer is 4 nm thick and reference (R) layer 2 nm thick. At remanence, they exhibit opposite chirality and aligned polarization. (b) Structure in which the storage and reference layers have the same thickness (3 nm). At remanence, the two vortices have the same chirality and polarization. (c) Hysteresis loop calculated by micromagnetic simulation for the structure of (b). Inset: The different configurations of magnetization under an in-plane external field. The aspect ratio of the disk appears here exaggerated due to the rectangular shape of meshes with $3 \times 3 \times 1$ nm.

procedure with the out-of-plane field application is mandatory to initialize it. The field necessary to reverse the reference-layer magnetization coming from positive saturation (after vortex annihilation, i.e., when this layer is close to the single-domain state) is approximately 20 mT.

The possibilities of multilevel storage using these two types of configurations (double vortex of opposite chirality or double vortex of the same chirality) are compared below.

In the configuration with the storage layer and reference layer in a vortex configuration of opposite chirality (storage layer 4 nm thick and reference layer 2 nm thick), the writing process is performed by cooling down the system from its blocking temperature to room temperature under 20 mT. After switching off the field, the storage-layer magnetization remains in a shifted vortex configuration [23] as illustrated in Fig. 3(a). For the reading process, ac currents 90∘ out of phase with a frequency of 200 MHz are supposed to be applied in the orthogonal word and bit lines, in order to generate an in-plane rotating field of amplitude 20 mT, enough to rotate the vortex core in the soft reference layer [Fig. 3(b)]. In MTJs, due to the TMR, the conductance varies as the cosine of the angle between the magnetization in the two magnetic electrodes. Here the two electrodes are in inhomogeneous magnetic states, so that a spatial integration must be performed of all local conductances to obtain the total MTJ conductance in a given configuration. The local conductances are given by the scalar product of the facing spins on both sides of the tunnel barrier. For convenience, we work in the following with the magnetoconductance (TMG) knowing that the conductance is just the inverse of the resistance. The advantage of the TMG is that it is a linear function of the integrated scalar product between the local magnetization in the two ferromagnetic electrodes. The expression of the normalized TMG is the following:

$$\mathrm{TMG} = \frac{\sum \mathbf{S}_{ir} \cdot \mathbf{S}_{ir}}{n}, \qquad (2)$$

where ir and is represent facing meshes from the reference and storage layer, respectively, in contact with the tunnel barrier, $\mathbf{S}_{ir}$ and $\mathbf{S}_{il}$ are the local magnetization orientations at these meshes, and n is the total number of meshes in a layer. The TMG as defined in Eq. (2) varies between −1 and 1 corresponding, respectively, to full antiparallel and parallel configurations. Snapshots of the storage- and reference-layer magnetization obtained during the application of the rotating field corresponding, respectively, to the situations of maximum and minimum conductances are presented in Figs. 3(a) and 3(b) together with the mapping of the local scalar products. The evolution of the TMG versus time is presented in Fig. 3(c).

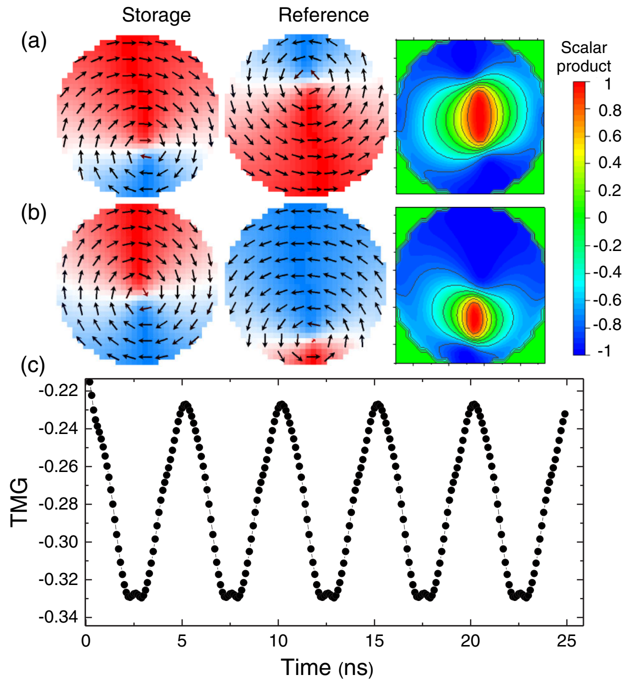

FIG. 3. Snapshot of magnetization in the pinned storage layer, reference-layer magnetization under a rotating field of 20 mT. (a) Configuration giving the maximum integrated scalar product between spins of both layers (maximum conductance), (b) configuration yielding the minimum integrated scalar product between spins of both layers (minimum conductance), and (c) evolution of the normalized TMG versus time.

From these results, it is possible in principle to derive the vortex position in the storage layer from the phase of the measured TMG signal. However, in this configuration where the two ferromagnetic layers have opposite vortex chirality, due to the relatively strong magnetostatic interactions between the two layers, the amplitude of the TMG signal is quite weak, of the order of only 5% of the full TMG signal. This value is too low for practical applications and would yield a long read access time.

We next turn to the configuration where the storage layer and reference layer have the same thickness (3 nm). In this case, two vortices of the same chirality can be stabilized by using the out-of-plane field-cooling procedure previously described. As a result, higher values of TMG can be expected, since almost full local parallel alignment can be obtained when the two vortices lie on top of each other.

However, as previously noted from the hysteresis loop, this configuration is very unstable. When applying the rotating external magnetic field to read out the information, even a small rotating field of 10 mT is enough to yield vortex annihilation in the reference layer after a few nanoseconds (less than one 360° rotation of the rotating field), as illustrated in Fig. 4(a). Figure 4(b) shows the time evolution of the TMG signal till the vortex annihilation. A variation close to 40% of TMG is obtained between the initial configuration and the vortex annihilation. The inset in Fig. 4(b) shows maps of the local scalar product (local conductance) in the initial configuration, wherein the

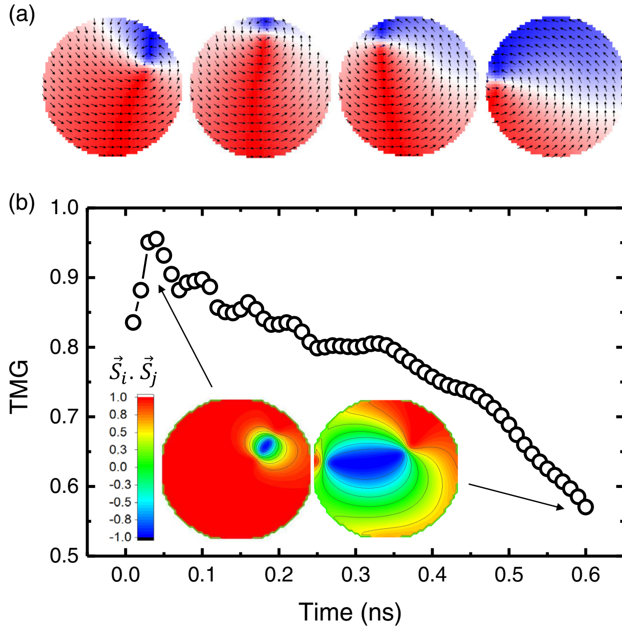

FIG. 4. Case where the storage layer and the reference layer have the same thickness (3 nm) and have been initialized with vortices of the same chirality and polarity. (a) Snapshots of vortex annihilation in the reference layer after from 0 s (left) to 0.6 ns (right) under a rotating field of 10 mT; red represents $+M_x$, blue $-M_x$, and white M_z. (b) TMG time variation from the initial configuration wherein the vortex cores are almost aligned to the configuration just before vortex annihilation in the reference layer. The inset shows maps of the local scalar product in the configurations yielding the highest and lowest conductance values.

vortex cores are almost aligned and just before the vortex annihilation.

In conclusion, the two configurations investigated in which the soft reference layer is in a vortex configuration do not seem very practical either, because they yield a quite low readout signal (case of vortices of opposite chirality) or because of the instability of the vortex configuration during operation (case of vortices of the same chirality).

An alternative option is to use a reference layer in the single-domain configuration. This is described in the following section.

B. Storage layer in vortex configuration and soft reference layer in single-domain configuration

In a second approach, the thickness of the soft reference layer and/or its initializing procedure are chosen to set this layer in a nearly uniform single-domain configuration. The magnetization is not strictly uniform due to the natural tendency of the magnetization to follow the pillar edges to minimize the magnetostatic energy. However, in the following, we call this state single domain for simplicity. In this case, after having applied the initializing protocol with out-of-plane field cooling to set the storage layer in the vortex state, an in-plane field of 20 mT is applied to annihilate the vortex which has been formed in the reference layer.

After these initializations, the write procedure consists as before in heating the storage layer above its AFM blocking temperature and cooling down the cell under a 20-mT magnetic field. This results in a transverse shift of the storage-layer vortex core.

We first consider the cells in which the storage layer and reference layer have the same thickness (3 nm).

In this case, due to the strong magnetostatic field created by the single-domain reference layer on the storage layer during the field-cooling procedure, the field cooling of the storage-layer magnetization must be realized quite fast to avoid vortex annihilation during the cooling. In these simulations, the vortex state in the storage layer could be stabilized provided the heating and cooling procedure is faster than approximately 1 ns, which would be experimentally challenging. We see later that, by using a thinner soft reference, this condition is removed because of the reduced magnetostatic field created by the reference layer on the storage layer.

Figure 5 illustrates some results obtained under these conditions. Different radial positions of the vortex core in the storage layer could be obtained by varying the heating and cooling pulse duration to freeze the vortex at various positions in its motion toward the edge. Several angular positions could also be obtained by varying the applied field directions, illustrated in Fig. 5(c) by using H_x or H_y applied fields.

In order to extract the stored information contained in the amplitude and phase of the TMG readout signal, a Fourier transform of the TMG signal is performed for each vortex core position. The graph presented in Fig. 6(a) shows the amplitude and phase extracted after 25 ns of reading for different vortex core positions obtained in the conditions of Fig. 5(c) with the field applied along in-plane x and y axes and along their diagonal (45°). For a given direction of the applied field, a shift of the phase of the core by about 20° is observed as the vortex core is set further off center. This is due to the dynamic motion of the core during the heating and cooling pulse under the influence of the applied field and stray field from the reference layer. As the angular shift of the phase is the same for all written directions at each field value, this phase shift in principle does not affect how many states can be written. Concerning the TMG signal amplitude, it is interesting to note that the obtained amplitudes are much larger here than in the case where the reference layer is also in the vortex configuration. In the present case, the calculated difference of about 15% between the normalized TMG amplitude obtained in the five radial positions tested and two angular positions per quadrant opens the possibility to obtain more than 40 states, represented in Fig. 6(b), in the same bit cell.

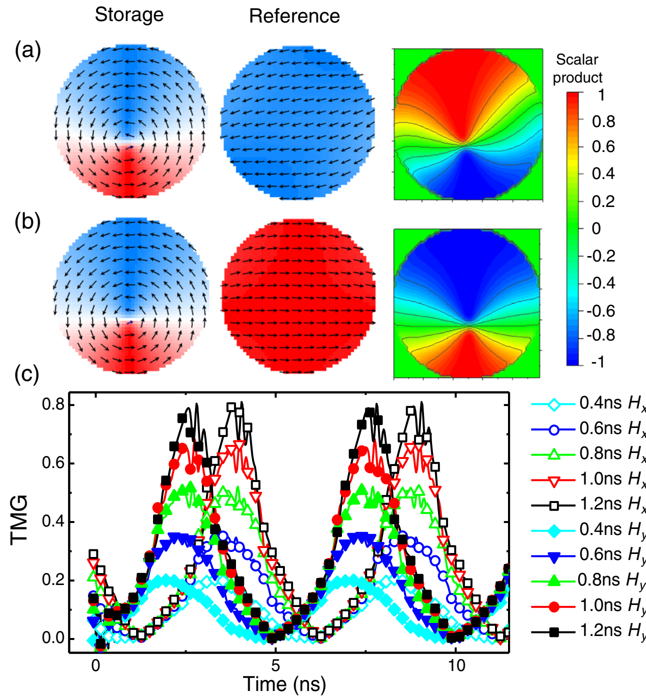

FIG. 5. Case of a storage layer in the vortex configuration and a reference layer in the single-domain configuration, both 3 nm thick. Snapshots of magnetization in the storage layer and reference layer under a rotating read field with the (a) configuration yielding maximum and (b) minimum average scalar product between spins of both layers. (c) Evolution of TMG signal versus time for different initial radial and angular positions of the vortex core obtained by varying the heating time between 0.4 and 1.2 ns and field application directions [H_x (open dots) and H_y (closed dots)].

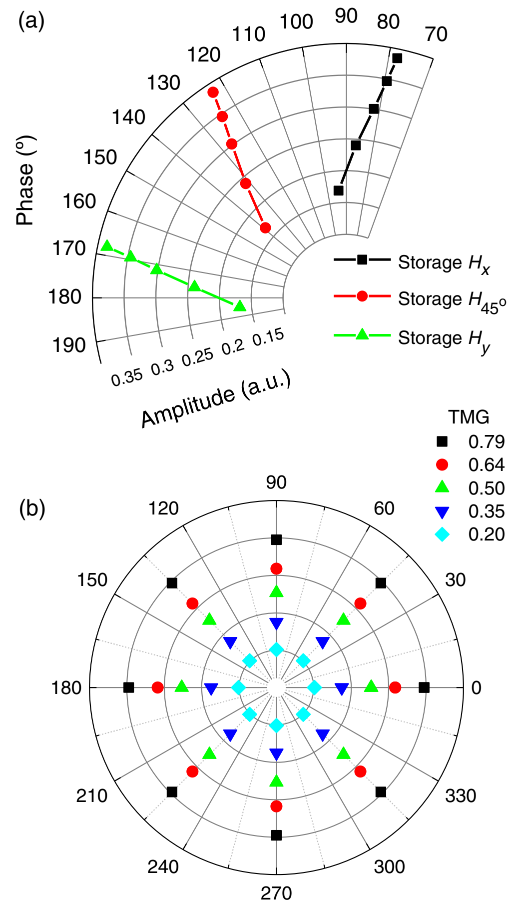

FIG. 6. (a) Amplitude and phase calculated by Fourier transform of the TMG signal presented in Fig. 5(c). (b) Different schematic possible stored states representing the set vortex core positions in the storage layer at remanence and corresponding TMG amplitude depending on the radial position.

As mentioned previously, due to the strong magnetostatic field created by the reference layer in the single-domain state on the storage layer when these two layers are 3 nm thick, the heating and cooling pulse during write must be quite short ($< \sim 1$ ns) to avoid the vortex annihilation in the storage layer. This would be rather difficult to implement experimentally, since, in typical TA MRAM, the heating and cooling phase typically lasts for 10 ns. In order to decrease the dipolar influence of the reference layer on the storage layer, a straightforward approach consists in reducing the thickness of the reference layer. In the following, the reference-layer thickness is decreased to 1.2 nm. Simulations are performed with the same parameters as before, just with the mesh size changed to $3 \times 3 \times 0.3$ nm. After applying the initial protocol to generate a vortex in the storage layer, the observed magnetization ground state is directly in-plane single-domain state magnetization in the reference layer and pinned vortex in the storage layer with the core slightly shifted due to the dipolar interaction with the reference layer [see Fig. 7(a)]. In order to further reduce the magnetostatic influence of the reference layer on the storage layer, a SAF reference layer is then used. The reference layer now consists of two antiferromagnetically coupled CoFe layers separated by a 0.9-nm Ru spacer providing an antiferromagnetic RKKY exchange coupling assumed to be equal to 1 mJ/cm^2. The use of different CoFe layer thicknesses in the two layers constituting the SAF (1.2 nm for the layer closest to the storage layer and 1.8 nm for the other layer) allows decreasing the dipolar interaction with the storage layer while maintaining a net magnetization in the reference layer, which will be necessary for magnetization rotation, under an external rotating magnetic field, during the readout process. The remanent state obtained after the initializing protocol is presented in Fig. 7(b). The vortex core is now well centered due to the reduced magnetostatic interaction between the reference layer and storage layer. The simulation of storage and reading processes is the same as before, with a rotating field lowered to 10 mT. The vortex core is set at three different radial positions by applying a write cooling field of 4, 5, and 6 mT. Interestingly, due to the reduced magnetostatic interactions between the reference layer and storage layer, there is no more requirement in the heating and cooling pulse duration

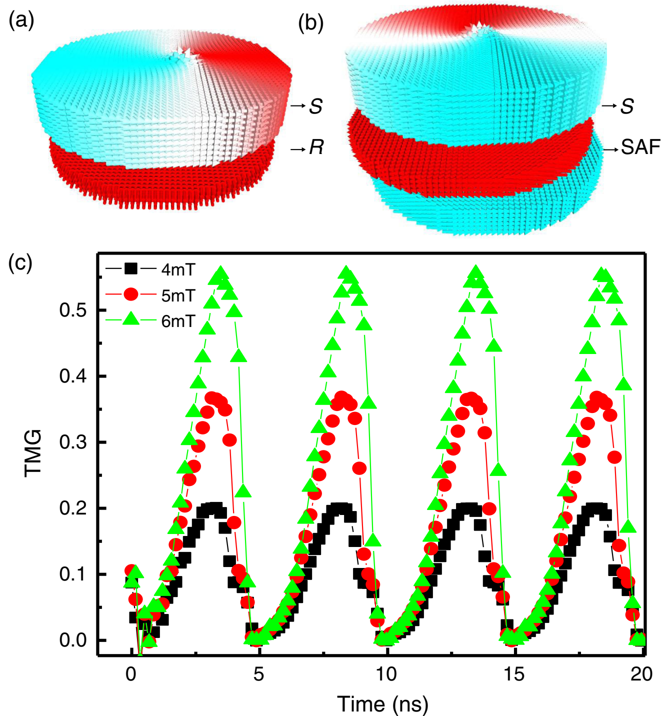

FIG. 7. Case where the storage layer is in a vortex configuration (3 nm thick) and a thinner reference layer in the single-domain state. (a) Remanent state when the reference layer consists of a single ferromagnetic layer 1.2 nm thick. A vortex shift in the storage layer is still observed due to the dipolar interaction with the reference layer. (b) Remanent state when the reference layer is part of a synthetic antiferromagnetic layer. The vortex in the storage layer is then centered in the initial state as a result of the reduced magnetostatic interaction with the SAF. (c) Time evolution of the TMG signal under the rotating read field of 10 mT for three radial positions of the storage-layer vortex core obtained by field cooling in $H_x = 4$, 5, and 6 mT.

to stabilize the vortex core position. The position of the vortex core in the storage layer can be set here as in conventional TA MRAM with a heating pulse of about 5–10 ns. The obtained TMG signals under a 10-mT rotating read field are shown in Fig. 7(c). Since the vortices are written here in a quasistatic way and not in a dynamic way as before, no more shift in the vortex core angular position is observed as the radial off centering of the core is increased. In addition, during the rotation of the soft reference-layer magnetization, the vortex in the storage layer remains almost fixed, which increases its stability upon reading. Because of these advantages, this configuration looks the most appropriate for implementation in practical devices.

III. CONCLUSION

We propose and investigate by micromagnetic simulations an approach for multilevel TA-MRAM design. It is based on the use of an exchange-biased storage layer in a vortex configuration. The information is encoded via the position of the vortex core which can be varied along two degrees of freedom: the radius and the angular position. Various configurations are studied and their advantages and drawbacks discussed. The most promising one among those investigated is one comprising a synthetic antiferromagnetic reference layer in a single-domain configuration in which the thicknesses of the two antiferromagnetically coupled ferromagnetic layers are adjusted to minimize the stray field on the storage layer. This configuration enables storage and writing under magnetic fields below 10 mT. From the results obtained in these simulations, the proposed TA MRAM could support more than 40 different logic states, corresponding to at least five bits per cell.

ACKNOWLEDGMENTS

This work is partly funded under ERC Advanced Grant No. 669204 MAGICAL and Brazilian agency CNPq.

[1] T. Miyazaki and N. Tezuka, Giant magnetic tunneling effect in $Fe/Al_2O_3/Fe$ junction, J. Magn. Magn. Mater. **139**, L231 (1995).

[2] J. S. Moodera, Lisa R. Kinder, Terrilyn M. Wong, and R. Meservey, Large Magnetoresistance at Room Temperature in Ferromagnetic Thin Film Tunnel Junctions, Phys. Rev. Lett. **74**, 3273 (1995).

[3] A. Khvalkovskiy, D. Apalkov, S. Watts, R. Chepulskii, R. S. Beach, A. Ong, X. Tang, A. Driskill-Smith, W. H. Butler, P. B. Visscher, D. Lottis, E. Chen, V. Nikitin, and M. Krounbi, Basic principles of STT-MRAM cell operation in memory arrays, J. Phys. D **46**, 074001 (2013).

[4] L. Savtchenko, B. N. Engel, N. D. Rizzo, M. DeHerrera, and J. Janesky, Method of writing to scalable magnetoresistance random access memory element, U.S. Patent No. 6,545,906 (8 April 2003).

[5] J. M. Slaughter, N. D. Rizzo, F. B. Mancoff, R. Whig, K. Smith, S. Aggarwal, and S. Tehrani, Toggle and spin-torque MRAM: Status and outlook, J. Magn. Soc. Jpn. **5**, 171 (2010).

[6] I. L. Prejbeanu, M. Kerekes, R. C. Sousa, H. Sibuet, O. Redon, B. Dieny, and J. P. Nozières, Thermally assisted MRAM, J. Phys. Condens. Matter **19**, 165218 (2007).

[7] I. L. Prejbeanu, W. Kula, K. Ounadjela, R. C. Sousa, O. Redon, B. Dieny, and J.-P. Nozieres, Thermally assisted switching in exchange-biased storage layer magnetic tunnel junctions, IEEE Trans. Magn. **40**, 2625 (2004).

[8] B. Dieny, R. Sousa, S. Bandiera, M. Castro Souza, S. Auffret, B. Rodmacq, J. P. Nozieres, J. Hérault, E. Gapihan, I. L. Prejbeanu, C. Ducruet, C. Portemont, K. Mackay, and B. Cambou, Extended scalability and functionalities of MRAM based on thermally assisted writing, IEEE Int. Electron. Devices Meet. **33**, 11 (2011).

[9] J. C. Slonczewski, Current-driven excitation of magnetic multilayer, J. Magn. Magn. Mater. **159**, L1 (1996).

[10] L. Berger, Emission of spin waves by a magnetic multilayer traversed by a current, Phys. Rev. B **54**, 9353 (1996).

[11] Y. Huai, F. Albert, P. Nguyen, M. Pakala, and T. Valet, Observation of spin-transfer switching in deep submicron-sized and low-resistance magnetic tunnel junctions, Appl. Phys. Lett. **84**, 3118 (2004).

[12] K. C. Chun, H. Zhao, J. Harms, T. H. Kim, J. P. Wang, and C. Kim, A scaling roadmap and performance evaluation of in-plane and perpendicular MTJ based STT-MRAMs for high-density cache memory, IEEE J. Solid State Circ. **48**, 598 (2013).

[13] W. S. Zhao, Y. Zhang, T. Devolder, J. O. Klein, D. Ravelosona, C. Chappert, and P. Mazoyer, Failure and reliability analysis of STT-MRAM, Microelectron. Reliab. **52**, 1848 (2012).

[14] I. M. Miron *et al.*, Current-driven spin torque induced by the Rashba effect in a ferromagnetic metal layer, Nat. Mater. **9**, 230 (2010).

[15] I. M. Miron, K. Garello, G. Gaudin, P.-J. Zermatten, M. V. Costache, S. Auffret, S. Bandiera, B. Rodmacq, A. Schuhl, and P. Gambardella, Perpendicular switching of a single ferromagnetic layer induced by in-plane current injection, Nature (London) **476**, 189 (2011).

[16] L. Liu, O. J. Lee, T. J. Gudmundsen, D. C. Ralph, and R. A. Buhrman, Current Induced Switching of Perpendicularly Magnetized Magnetic Layers Using Spin Torque from the Spin Hall Effect, Phys. Rev. Lett. **109**, 096602 (2012).

[17] M. Cubukcu, O. Boulle, M. Drouard, K. Garello, C. O. Avci, I. M. Miron, J. Langer, B. Ocker, P. Gambardella, and G. Gaudin, Spin-orbit torque magnetization switching of a three-terminal perpendicular magnetic tunnel junction, Appl. Phys. Lett. **104**, 042406 (2014).

[18] K. Garello, C. O. Avci, I. M. Miron, M. Baumgartner, A. Ghosh, S. Auffret, O. Boule, G. Gaudin, and P. Gambardella, Ultrafast magnetization switch by spin orbit torques, Appl. Phys. Lett. **105**, 212402 (2014).

[19] T. Ishigaki, T. Kawahara, R. Takemura, K. Ono, K. Ito, H. Matsuoka, and H. Ohno, in *Proceedings of the 2010 Symposium on VLSI Technology* (IEEE, New York, 2010), pp. 234–235.

[20] I. L. Prejbeanu, Multibit magnetic random access memory cell with improved read margin, U.S. Patent No. 20120155159 (21 June 2012).

[21] Q. Stainer, L. Lombard, K. Mackay, D. Lee, S. Bandiera, C. Portemont, C. Creuzet, R. C. Sousa, and B. Dieny, Self-referenced multi-bit thermally assisted magnetic random access memories, Appl. Phys. Lett. **105**, 032405 (2014).

[22] K. L. Metlov and Y. Lee, Map of metastable states for thin circular magnetic nanocylinders, Appl. Phys. Lett. **92**, 112506 (2008). Note: In the present paper, we use as the exchange length the standard expression in SI units given by $L_{\rm ex} = \sqrt{2A_{\rm ex}/\mu_0 M_s^2}$ (see http://ieeexplore.ieee.org/stamp/stamp.jsp?arnumber=6497624), whereas this reference uses as the definition $L_{\rm ex} = \sqrt{4\pi A_{\rm ex}/\mu_0 M_s^2}$. Therefore, the data of Ref. [22] are transformed according to the standard definition of $L_{\rm ex}$ for discussion in this paper.

[23] J. Sort, K. S. Buchanan, V. Novosad, A. Hoffman, G. Salazar-Alvarez, A. Bollero, M. D. Baró, B. Dieny, and J. Nogués, Imprinting Vortices into Antiferromagnets, Phys. Rev. Lett. **97**, 067201 (2006).

[24] A. Vansteenkiste, J. Leliaert, M. Dvornik, M. Helsen, F. G. Sanchez, and B. V. Waeyenberge, The design and verification of MuMax3, AIP Adv. **4**, 107133 (2014).

[25] K. Tanahashi, A. Kikukawa, and Y. Hosoe, Exchange-biased CoTaZr soft underlayer for perpendicular recording, J. Appl. Phys. **93**, 8161 (2003).

[26] K. Yu. Guslienko, V. Novosad, Y. Otani, H. Shima, and K. Fukamichi, Field evolution of magnetic vortex state in ferromagnetic disks, Appl. Phys. Lett. **78**, 3848 (2001).

[27] P. Wiśniowski, J. M. Almeida, S. Cardoso, N. P. Barradas, and P. P. Freitas, Effect of free layer thickness and shape anisotropy on the transfer curves of MgO magnetic tunnel junctions, J. Appl. Phys. **103**, 07A910 (2008).